THE JOURNAL OF BIOLOGICAL CHEMISTRY VOL. 289, NO. 19, pp. 13638–13650, May 9, 2014


# βArrestin1 Regulates the Guanine Nucleotide Exchange Factor RasGRF2 Expression and the Small GTPase Rac-mediated Formation of Membrane Protrusion and Cell Motility*

Received for publication, August 23, 2013, and in revised form, March 28, 2014 Published, JBC Papers in Press, April 1, 2014, DOI 10.1074/jbc.M113.511360

**Xiaojie Ma, Laura Espana-Serrano, Wan-ju Kim, Hamsa Thayele Purayil, Zhongzhen Nie[1], and Yehia Daaka**

*From the ‡Department of Anatomy and Cell Biology, University of Florida College of Medicine, Gainesville, Florida 32610*

**Background:** G protein-coupled receptors (GPCRs) and βarrestins have been shown to regulate cell motility.
**Results:** βArrestin1 regulates cell migration through RasGRF2 (a dual guanine nucleotide exchange factor) gene expression and the small GTPase Rac activity.
**Conclusion:** βArrestin1 may regulate cellular functions at the gene expression level.
**Significance:** βArrestins may function at transcriptional and post-translational levels to regulate cell migration.

**βArrestin proteins shuttle between the cytosol and nucleus and have been shown to regulate G protein-coupled receptor signaling, actin remodeling, and gene expression. Here, we tested the hypothesis that βarrestin1 regulates actin remodeling and cell migration through the small GTPase Rac. Depletion of βarrestin1 promotes Rac activation, leading to the formation of multipolar protrusions and increased cell circularity, and overexpression of a dominant negative form of Rac reverses these morphological changes. Small interfering RNA library screen identifies RasGRF2 as a target of βarrestin1. RasGRF2 gene and protein expression levels are elevated following depletion of βarrestin1, and the consequent activation of Rac results in dephosphorylation of cofilin that can promote actin polymerization and formation of multipolar protrusions, thereby retarding cell migration and invasion. Together, these results suggest that βarrestin1 regulates *rasgrf2* gene expression and Rac activation to affect membrane protrusion and cell migration and invasion.**

Cell migration and invasion are multistep processes that require actin cytoskeleton remodeling and the establishment and maintenance of cell polarity (1). Rac is a Rho GTPase family member that regulates actin remodeling and protrusive structures at the leading edge of migrating cells. Activation of Rac through GTP binding is catalyzed by guanine nucleotide exchange factors (GEFs),[2] which can be divided into two subfamilies as follows: those that contain the Dbl homology-pleckstrin homology and those that contain Dock homology region domains (2, 3). RasGRF2 is a multidomain protein that has dual Ras GEF and Rac GEF activities. The Cdc25 homology domain at the C terminus catalyzes exchange of GDP to GTP on Ras family proteins, whereas the Dbl homology-pleckstrin homology domain functions as a GEF for Rac proteins (4). RasGRF2 was initially identified in neuronal tissues, and its known functions in the nervous system include regulation of NMDA receptor signaling and synaptic plasticity (5). Although mechanisms underlying the restricted tissue distribution of RasGRF2 are not fully understood, recent studies have suggested that RasGRF2 expression is suppressed in different human cancers, implying a tumor suppressive role (4), but by as yet unclear mechanisms.

βArrestins, including βarrestin1 (βArr1 also known as Arr2) and βArr2 (also known as Arr3), were initially characterized based on their ability to regulate G protein-coupled receptor (GPCR) signaling (6), and they have been implicated in human cancers (7–10). Emerging evidence shows that βArr1 and βArr2 also function as adaptors to transduce signals and to regulate a wide array of cellular functions, including actin remodeling and cell migration (11, 12). One mechanism by which βArrs regulate actin remodeling and cell migration is through regulation of monomeric G proteins, including RhoA, Cdc42, and RalA. For example, activation of angiotensin II type 1A receptor resulted in RhoA activation that is dependent upon βArr1, leading to stress-fiber formation (13). The type III transforming growth factor receptor, whose expression is lost in many human cancers, inhibits cell migration through βArr2-mediated activation of Cdc42 (14). βArr1 was also shown to form a complex with Ral-guanine dissociation stimulator in the cytosol, and upon activation of formylmethionylleucylphenylalanine or lysophosphatidic acid receptors, RalA was activated resulting in actin remodeling and cell migration (15).

GPCRs and βArrs have been shown to regulate Rho GTPases through either RhoGEFs or RhoGAPs (GTPase-activating proteins). Activation of the angiotensin II type 1A receptor facilitated association of βArr1 with the RhoGAP ARHGAP21, and consequent inhibition of the GTPase-activating proteins contributed to higher RhoA activity (16). Angiotensin II type 1A receptor was also shown to mediate RhoA activation through both βArr1 and $G_q$ (13), as well as through JAK2-mediated

* This work was supported, in whole or in part, by National Institutes of Health Grants K22CA124578 from USPHS (to Z. N.) and R01CA129155 from NCI (to Y. D.).
[1] To whom correspondence should be addressed: Division of Cell Biology and Biophysics, NIGMS, National Institutes of Health, 45 Center Dr., Rm. 2AS13H, MSC6200, Bethesda, MD 20892. E-mail: niezhong@nigms.nih.gov.
[2] The abbreviations used are: GEF, guanine nucleotide exchange factor; GPCR, G protein-coupled receptor; MEF, mouse embryonic fibroblast; RFP, red fluorescent protein; βArr, βarrestin1; RCC, renal cell carcinoma.

phosphorylation of p115RhoGEF (17). We recently reported that βArr2 formed a complex with p115RhoGEF in the cytosol and that activation of the $\beta_2$adrenergic receptor resulted in membrane translocation and activation of p115RhoGEF and RhoA (18).

Here, we report the regulation of RasGRF2 expression by βArr1. Depletion of βArr1 resulted in higher expression of RasGRF2 and higher Rac activity, leading to the formation of multipolar protrusions and cell rounding. Consistent with increased actin polymerization, depletion of βArr1 was associated with lower levels of cofilin phosphorylation, reflecting higher cofilin activity. Knockdown of RasGRF2 expression with siRNA increased cofilin phosphorylation in $\beta Arr1^{-/-}$, but not $\beta Arr1^{+/+}$, mouse embryonic fibroblasts (MEFs), which was reversed by Rac inhibition. Overexpression of a RasGRF2 mutated form with a deleted Ras GEF domain was sufficient to cause cofilin dephosphorylation, supporting the idea that higher Rac activity is responsible for the βArr1-dependent regulation of cofilin. Chromatin immunoprecipitation results indicated that βArr1 bound to the promoter region of *rasgrf2*, and treatment with the demethylating agent decitabine enhanced *rasgrf2* gene expression. In agreement with the formation of multipolar protrusions and loss of unipolarity, depletion of βArr1 resulted in the reduced rate of directional cell migration and invasion. Therefore, βArr1 regulates Rac activity and membrane protrusions through, at least in part, RasGRF2-related mechanisms.

## MATERIALS AND METHODS

*Cell Culture and Reagents*—Mouse embryonic fibroblasts (MEFs) and HEK293 cells were cultured in Dulbecco's modified Eagle's medium (DMEM) supplemented with 10% fetal bovine serum (FBS) (Hyclone), 100 units/ml penicillin, and 100 μg/ml streptomycin (Mediatech). Caki-1, SN12C, and RCC7 renal carcinoma cells were maintained in RPMI 1640 medium supplemented with 10% FBS, penicillin, and streptomycin. All cells were grown at 37 °C in a humidified 5% $CO_2$ incubator. pEGFP-N1, pEGFP-N1-Rac, pEGFP-N1-T17N-Rac, and pEGFP-N1-Q61L-Rac were obtained from Addgene. pcDNA-FLAG-RasGRF2 and pcDNA3-FLAG-ΔCdc25-RasGRF2 were gifted by Dr. P. Crespo (University of Cantabria). Adenoviruses encoding βArr1 were provided by Dr. W. Koch (Temple University). Antibodies were obtained as follows: anti-βarrestin1, anti-ERK2, and anti-mouse RasGRF2 from Santa Cruz Biotechnology; anti-βarrestin1/2, anti-cofilin, anti-phospho-ERK, and anti-phospho-cofilin (Serine 3) from Cell Signaling; anti-human RasGRF2 from Abcam; and A1CT anti-βarrestin gifted by Dr. R. J. Lefkowitz (Duke University). Rhodamine-conjugated phalloidin was from Invitrogen, and FITC- or rhodamine-conjugated secondary antibodies were from Jackson ImmunoResearch.

*Transfection and Immunofluorescence*—$\beta Arr1^{+/+}$ and $\beta Arr1^{-/-}$ MEFs (kind gift from Dr. R. J. Lefkowitz) were transfected using GenJet (SignaJen), and RCC7 cells were transfected using PEI (Polysciences Inc.). Gene knockdown using SMARTpool siRNAs (Dharmacon) targeting specific Rac GEFs was performed using Lipofectamine RNAiMax (Invitrogen). Stable knockdown of βArr1 in RCC7 cells was achieved by transfection of shRNA constructs (Open Biosystems) in lentiviral pLKO vector plus an equal concentration of vesicular stomatitis virus G and Δ8.9 vector into packaging HEK293T cells for 24 and 48 h. Lentivirus containing medium was harvested, mixed with Polybrene, and used to infect RCC7 cells. The infected polyclonal cells were selected with 2 μg/ml puromycin for 2 weeks. To restore βArr1 expression, $\beta Arr1^{-/-}$ MEFs were infected with adenoviruses encoding βArr1, and infection with adenoviruses encoding RFP was used as a control.

For immunofluorescence staining, cells were trypsinized and replated onto fibronectin-coated coverslips, incubated in Opti-MEM or other medium (as indicated) for 6 h, and fixed with 2% formaldehyde. Actin cytoskeleton was visualized by staining with rhodamine-conjugated phalloidin. Slides were examined using an epifluorescence microscope (DM 6000B, Leica) equipped with a ×63/1.4-0.6 oil immersion lens or a Leica confocal microscope (TCS SP5) equipped with ×63/1.4 NA oil immersion lens. Images were captured and analyzed using the Volocity software 5.5 (PerkinElmer Life Sciences) or the application suite Advanced Fluorescence 2.0.2 software (Leica). For protrusion numbers, at least 100 control or knock-out MEFs were counted for each assay, and the experiments were repeated three times. For circularity measurement, the short axis and the long axis of each MEF were measured, and the circularity was expressed as the quotient of the short axis divided by the long axis. Hence, the lower value reflects elongated morphology, and the higher value indicates cell rounding.

*GST Pulldown*—GST, GST-CRIB (Cdc42/Rac-interactive binding domain of PAK), and GST-RBD (Rho binding domain of rhotekin) fusion proteins were expressed in BL21 cells. After induction with isopropyl 1-thio-β-D-galactopyranoside, cells were harvested by centrifugation and lysed in 1% Triton X-100 in PBS with protease inhibitors using a French pressure cell press. Cell lysates were centrifuged at 100,000 × *g* at 4 °C for 1 h, and the supernatants were incubated with glutathione-conjugated agarose beads at 4 °C for 1 h followed by washing with PBS. Fresh cell lysates (in 20 mM Tris, pH 8.0, 100 mM NaCl, 10% (v/v) glycerol, 1% (v/v) Triton X-100, 1 mM EDTA, 5 mM $MgCl_2$, 1 mM phenylmethylsulfonyl fluoride, 10 μg/ml aprotinin, 10 μg/ml leupeptin, and 2 μg/ml pepstatin A) were incubated with GST fusion proteins bound to beads with rotation at 4 °C for 1 h. The beads were washed three times and boiled in SDS-PAGE sample buffer. Precipitated proteins (*i.e.* GTP-bound Rac, Cdc42, or RhoA) were determined by Western blot.

*Cell Migration and Invasion*—Cell migration and invasion were examined using Boyden chambers. MEFs or renal cell carcinoma (RCC) cells were starved overnight in 0.2% (v/v) FBS medium and then detached using HyQTase (Thermo). A total of $2.5 \times 10^4$ MEFs or Caki-1 cells and $1.0 \times 10^5$ SN12C or RCC7 cells in 100 μl of medium containing 0.2% FBS were loaded into the top chamber. After 3 h of seeding, medium containing 0.5% FBS or PDGF (10 ng/ml) was added into the bottom chamber. For invasion assay, 1 mg/ml Matrigel (BD Biosciences) was thawed at 4 °C overnight and added onto the chamber filter at 37 °C for 1 h. Cell migration was terminated at 8 h for MEFs and 18 h for RCC, and cell invasion proceeded for 24 h. Cells were fixed and stained with Diff-Quik staining solution (Siemens).

Cells that remained in the top chamber were removed using a cotton swab, and the cells on the underside of the filter were photographed in four randomly chosen fields using the Leica DMI 4000B inverted microscope and counted using ImageJ software.

*Real Time PCR*—Decitabine (Sigma) treatment was performed as follows. Cells were cultured at low density for 24 h before decitabine was added at 1 μM for an additional 24 h. Cells were washed three times with PBS, and fresh medium was added for an additional 24 h. A total of three decitabine treatment cycles were performed prior to harvesting cells for quantitative RT-PCR. Total RNA was isolated using TRIzol (Invitrogen), and 2 μg of RNA was reverse-transcribed to generate cDNA using Superscript III (Invitrogen). Real time PCR was performed on Bio-Rad iQ5 thermal iCycler detection system using iQ™ SYBR Green SuperMix (Bio-Rad). Relative expression levels were calculated using the $\Delta\Delta C_t$ method, and actin was used as the internal control (7). Expression level of target genes was presented relative to the expression in control cells. The sense and antisense primers used were as follows: *tiam1* forward 5′-ATT GAA ATC TGT CCA AAA GTC ACT C-3′ and *tiam1* reverse 5′-TTC TTC CAC AGA AGA AAG TGA AAA C-3′; *arhgef6* forward 5′-TAT GGA GGA TAC TCA TCC AGA TCA T-3′ and *arhgef6* reverse 5′-CTG TAA CTC CAG CTG TTT TCT CTT C-3′; *dock4* forward 5′-TGG AGA TAC AGT TCA GAT CCT GGA G-3′ and *dock4* reverse 5′-TTT TTC AAG TGA ACG TAG CTG GAA G-3′; *rasgrf2* forward 5′-CCA ATT GTA AGC AAA ACA GAG ATT T-3′ and *rasgrf2* reverse 5′-TGA TAT ATC TGG GGA TCT GAA ACA T-3′; and *dock7* forward 5′-TCA CCT TCT GTT TCT TCT GCA A-3′ and *dock7* reverse 5′-ACA AGT CCT GCC AAA TAA TGC T-3′.

*Chromatin Immunoprecipitation (ChIP)*—ChIP assay was performed using EZ ChIP kit (Millipore) following the manufacturer's protocol. Briefly, both $\beta Arr1^{+/+}$ and $\beta Arr1^{-/-}$ MEFs were treated with 1% formaldehyde to cross-link the DNA and proteins. Glycine (1.25 M) was added into the medium to quench formaldehyde. Cells were lysed and sonicated (Covaris E210, set up to generate 400-bp DNA fragments) to generate cross-linked DNA fragments with an average size of 400 bp. Immunoprecipitation was done by incubating chromatin with A1CT antibody at 4 °C overnight. ChIP complex was eluted with elution buffer (1% SDS, 0.1 M $NaHCO_3$), and the cross-link was reversed using 5 M NaCl. DNA was purified using spin columns, and PCR amplification was performed using the purified DNA template and hot start Taq polymerase (Qiagen). The primers used were as follows: *rasgrf2* promoter forward 5′-ATA GGC GCC CTA GGT CTG G-3′ and *rasgrf2* promoter reverse 5′-GAG TCG TAG CCT CAG CTT CTT G; *p21* promoter forward 5′-CCA GAG GAT ACC TTG CAA GGC-3′ and *p21* promoter reverse 5′-TCT CTG TCT CCA TTC ATG CTC CTC C-3′.

*Statistical Analysis*—Experiments were repeated at least three times, and data are expressed as mean ± S.E. Statistical analysis was performed using Student's *t* test or one-way analysis of variance with Tukey's post hoc test. Graphs were generated using Prism (version 5.0), and axis labels were generated using Adobe Illustrator (version CS5) software, respectively.

## RESULTS

*βArr1 Regulates Cell Morphology and Rac Activity*—Deletion of βArr1 resulted in morphological changes of MEFs (18). As shown in Fig. 1*A*, *panels a* and *b*, $\beta Arr1^{+/+}$ MEFs were elongated with monopolar protrusions, whereas $\beta Arr1^{-/-}$ MEFs were less elongated and more flattened with multipolar protrusions (Fig. 1*A*, *panels c* and *d*). Quantification of protrusion numbers indicated that there were roughly three protrusions per $\beta Arr1^{+/+}$ MEF and six protrusions per $\beta Arr1^{-/-}$ MEF (Fig. 1*B*). We measured cell dimensions and found that $\beta Arr1^{+/+}$ MEFs exhibited low circularity in comparison with the $\beta Arr1^{-/-}$ MEFs (Fig. 1*C*), suggesting that deletion of βArr1 resulted in loss of unipolar morphology in a manner comparable with the loss of polarity of migratory T cells upon activation of T cell receptors (19). Similar results were obtained when MEFs were seeded on noncoated surfaces or cultured in the presence or absence of serum (data not shown). Hence, these morphological alterations are likely acquired properties irrespective of serum growth factor receptor or integrin receptor activation.

As membrane protrusions are regulated, at least in part, by Rho GTPases, we measured the level of active Rho GTPase in MEFs. Knock-out of βArr1 did not affect the average level of Cdc42·GTP (Fig. 1, *D* and *E*) with no noticeable effect on RhoA·GTP levels, as we have reported previously (18). Distinctly, $\beta Arr1^{-/-}$ MEFs showed elevated levels of Rac·GTP (Fig. 1*D*), and densitometry analysis indicated that deletion of βArr1 increased Rac activity by roughly 3-fold (Fig. 1*F*). To test the idea that the increased Rac activity was a direct result of βArr1 loss of expression, we restored expression of βArr1 in $\beta Arr1^{-/-}$ MEFs through infection with βArr1-encoding adenovirus (Fig. 1*G*). Rac activity decreased in MEFs with rescued βArr1 expression, as compared with $\beta Arr1^{-/-}$ MEFs infected with control RFP-encoding adenoviruses (Fig. 1*H*).

To provide further evidence that Rac activity increases upon depletion of βArr1, we compared the spreading of $\beta Arr1^{+/+}$ and $\beta Arr1^{-/-}$ MEFs on fibronectin-coated surfaces. $\beta Arr1^{+/+}$ MEFs were elongated with membrane ruffles after 30 min of spreading (Fig. 1*I*, *panels a* and *b*, *small arrows*), with very few MEFs forming lamellipodia (Fig. 1*I*, *panel b, big arrow*). In contrast, most of the $\beta Arr1^{-/-}$ MEFs formed lamellipodia at 30 min of spreading (Fig. 1*I*, *panels c* and *d*), suggesting higher Rac activity following deletion of βArr1.

*βArr1 Regulates MEF Morphology through Rac*—We examined whether Rac was involved in the morphological changes of $\beta Arr1^{-/-}$ MEFs. To this end, we transfected $\beta Arr1^{-/-}$ MEFs with expression vectors encoding GFP fusion proteins of wild-type (WT) Rac, (T17N)Rac that is deficient in GTP binding, or (Q61L)Rac that is deficient in GTP hydrolysis. GFP-transfected $\beta Arr1^{-/-}$ MEFs (Fig. 2*A*, *panels a–d*), like GFP-Rac- (Fig. 2*A*, *panels e–h*) or GFP-(Q61L)Rac (Fig. 2*A*, *panels i–l*)-transfected $\beta Arr1^{-/-}$ MEFs exhibited multipolar protrusions and increased circularity, suggesting that basal Rac activity was sufficiently high to induce the morphological changes. Remarkably, overexpression of dominant negative GFP(T17N)Rac

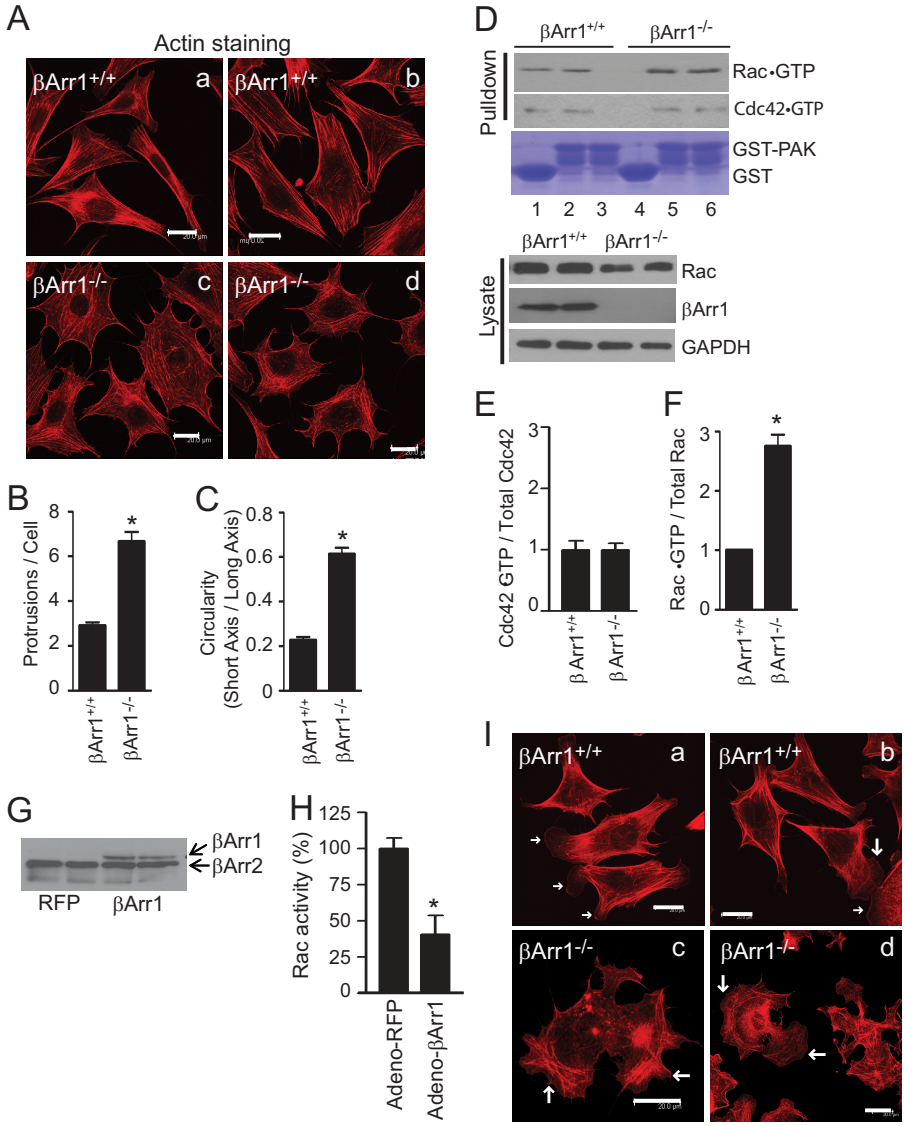


FIGURE 1. ***βArr1 regulates cell morphology and Rac activity.*** *A,* depletion of βArr1 impacts protrusion formation and cell rounding. $\beta Arr1^{+/+}$ and $\beta Arr1^{-/-}$ MEFs were trypsinized and seeded onto fibronectin-coated coverslips for 6 h in Opti-MEM. Cells were fixed and stained with rhodamine-conjugated phalloidin. $\beta Arr1^{+/+}$ MEFs were elongated with unipolar morphology, whereas $\beta Arr1^{-/-}$ MEFs formed multipolar protrusions with rounding. *B* and *C,* quantification of the protrusion numbers (*B*) and circularity (*C*) of $\beta Arr1^{+/+}$ and $\beta Arr1^{-/-}$ MEFs. *, $p < 0.05$ *versus* $\beta Arr1^{+/+}$ MEFs. *D,* measurement of Rac·GTP level and Cdc42·GTP in $\beta Arr1^{+/+}$ and $\beta Arr1^{-/-}$ MEFs by GST-CRIB (of PAK) pulldown. *Top panels* show pulldown results of Rac and Cdc42 by Western blot, with Coomassie Blue staining of GST and GST-PAK shown *below* the Western blots. Note that control pulldown with GST was shown in *lanes 1* and *4*, whereas pulldown of active Rac with GST-PAK was performed in duplicate as shown in *lanes 2* and *3* and *lanes 5* and *6*. *Bottom panels* show total Rac and βArr1 in cell lysates, using GAPDH as a loading control. *E,* quantification of Cdc42·GTP level as normalized to total Cdc42 by densitometry. *F,* quantification of Rac·GTP level as normalized to total Rac by densitometry. *, $p < 0.05$ *versus* $\beta Arr1^{+/+}$ MEFs. *G* and *H,* restored expression of βArr1 decreases Rac activity. $\beta Arr1^{-/-}$ MEFs were infected with adenoviruses encoding RFP or βArr1. Cell lysates were prepared, and rescued βArr1 protein levels were detected by Western blot (*G*), and active Rac levels by pulldown (*H*) assays. *, $p < 0.05$ *versus* control adeno-RFP-infected $\beta Arr1^{-/-}$ MEFs. *I,* spreading of MEFs. $\beta Arr1^{+/+}$ and $\beta Arr1^{-/-}$ MEFs were seeded on fibronectin-coated coverslips for 30 min and stained with rhodamine-conjugated phalloidin. *Small arrows* indicate membrane ruffles, and *big arrows* indicate lamellipodium. *Scale bars,* 20 μm.

reversed the multipolar morphology of $\beta Arr1^{-/-}$ MEFs (Fig. 2*A*, *panels m–p*). MEFs that express (T17N)Rac showed elongated morphology with fewer protrusions. These results support the idea that higher Rac activity mediates the morphological changes of $\beta Arr1^{-/-}$ MEFs.

We quantified protrusion numbers in $\beta Arr1^{+/+}$ and $\beta Arr1^{-/-}$ MEFs with or without overexpression of GFP fusion proteins of WT or mutated Rac. $\beta Arr1^{+/+}$ MEFs transfected with control GFP alone exhibited about two protrusions per MEF, and overexpression of GFP-Rac or GFP-(T17N)Rac did not change the protrusion numbers (Fig. 2*B*). However, expression of GFP-(Q61L)Rac significantly increased the protrusion number (Fig. 2*B*). $\beta Arr1^{-/-}$ MEFs transfected with control GFP presented with over five protrusions per MEF, which was not affected by overexpression of GFP-Rac or GFP-(Q61L)Rac (Fig. 2*B*). Distinctly, the expression of dominant negative GFP-(T17N)Rac significantly reduced protrusion number in $\beta Arr1^{-/-}$ MEFs (Fig. 2*B*). Measurement of dimensions indicated similar effects of Rac on MEF circularity; overexpression of GFP-(Q61L)Rac increased circularity of $\beta Arr1^{+/+}$ MEFs, although overexpression of GFP-(T17N)Rac reduced circularity of $\beta Arr1^{-/-}$ MEFs (Fig. 2*C*). Taken together, these results suggest that higher Rac

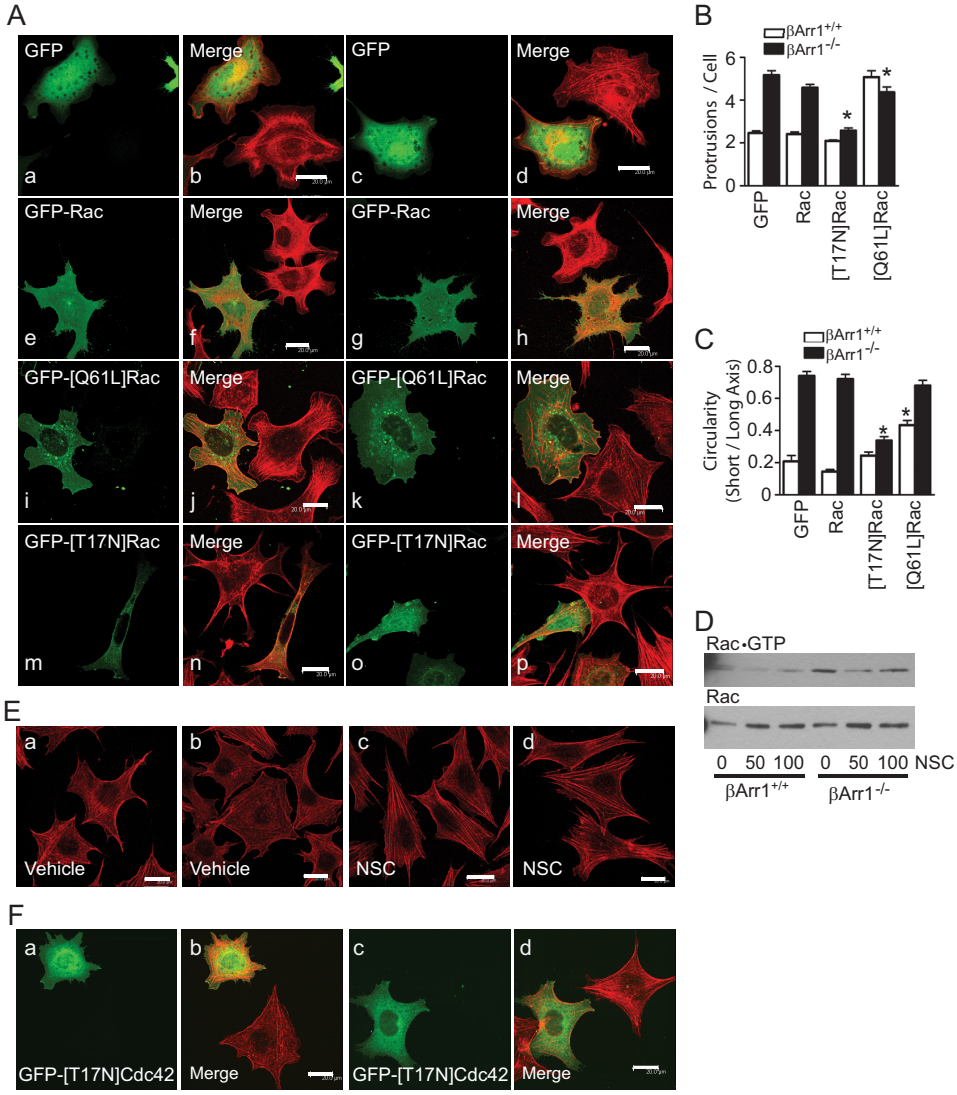


FIGURE 2. **βArr1 regulates multipolar protrusions and cell circularity through Rac.** *A,* βArr1$^{-/-}$ MEFs were transfected with expression vectors for GFP (*panels a–d*), GFP-Rac (*panels e–h*), GFP-(Q61L)Rac (*panels i–l*), or GFP-(T17N)Rac (*panels m–p*) for 24 h. MEFs were reseeded on fibronectin-coated coverslips for 6 h, fixed, and stained with rhodamine-conjugated phalloidin. Slides were examined using confocal microscopy. Images are shown for GFP or merged GFP and actin staining. *B,* quantification of protrusion numbers of βArr1$^{+/+}$ and βArr1$^{-/-}$ MEFs ectopically expressing Rac or its mutated forms. *, $p < 0.05$ *versus* GFP vector control. *C,* measurement of circularity of βArr1$^{+/+}$ and βArr1$^{-/-}$ MEFs ectopically expressing WT or mutated Rac. *, $p < 0.05$ *versus* GFP vector control. *D,* NSC23766 inhibited Rac activation. βArr1$^{+/+}$ and βArr1$^{-/-}$ MEFs were treated with NSC23766 (*NSC*) (50 or 100 μM) or vehicle for 18 h in starvation medium, followed by stimulation with PDGF (10 ng/ml) for 5 min. Rac·GTP level was determined by pulldown. *E,* Rac inhibition alters βArr1$^{-/-}$ MEF morphology. βArr1$^{-/-}$ MEFs were treated with NSC23766 (50 μM) for 48 h, reseeded on fibronectin-coated coverslips for 6 h, and stained with rhodamine-conjugated phalloidin. *F,* (T17N)-Cdc42 has no effect on βArr1$^{-/-}$ MEF morphology. βArr1$^{-/-}$ MEFs were transiently transfected with GFP-(T17N)Cdc42, and cell morphology was examined by actin staining. *Scale bars,* 20 μm.

activity is involved in multipolar protrusion formation and rounding of βArr1$^{-/-}$ MEFs.

To gain more confidence in the involvement of Rac, we treated βArr1$^{-/-}$ MEFs with the known Rac inhibitor NSC23766 (20, 21) and examined the effects on cell morphology. Treatment with NSC23766 decreased active Rac levels in both βArr1$^{+/+}$ and βArr1$^{-/-}$ MEFs (Fig. 2*D*). Rac inhibition effectively altered βArr1$^{-/-}$ MEFs morphology from rounded with multiple protrusions (Fig. 2*E*, *panels a* and *b*) to elongated with fewer protrusions (Fig. 2*E*, *panels c* and *d*).

As Cdc42 also plays critical roles in the regulation of cell morphology, we examined whether overexpression of dominant negative Cdc42 affects βArr1$^{-/-}$ MEFs. Following overexpression of GFP-(T17N)Cdc42, βArr1$^{-/-}$ MEFs remained rounded with multiple protrusions (Fig. 2*F*, *panels a–d*), suggesting that Cdc42 is less likely to be involved in the regulation of βArr1$^{-/-}$ MEF morphology.

*βArr1/Rac Signaling Negatively Regulates Activity of Cofilin*—Cofilin is an actin-binding and -severing protein that increases the number of free barbed ends to promote actin polymerization and formation of actin-rich protrusions. Cofilin activity is regulated by phosphorylation; phosphorylation of the serine 3 residue inhibits cofilin's actin-severing capacity, although its dephosphorylation results in the cofilin activation. βArr1$^{-/-}$ MEFs formed multipolar protrusions, suggesting a high rate of actin polymerization. Accordingly, knock-out of βArr1 resulted in dephosphorylation of cofilin (Fig. 3*A*). Densitometry analysis revealed that there was a 75%

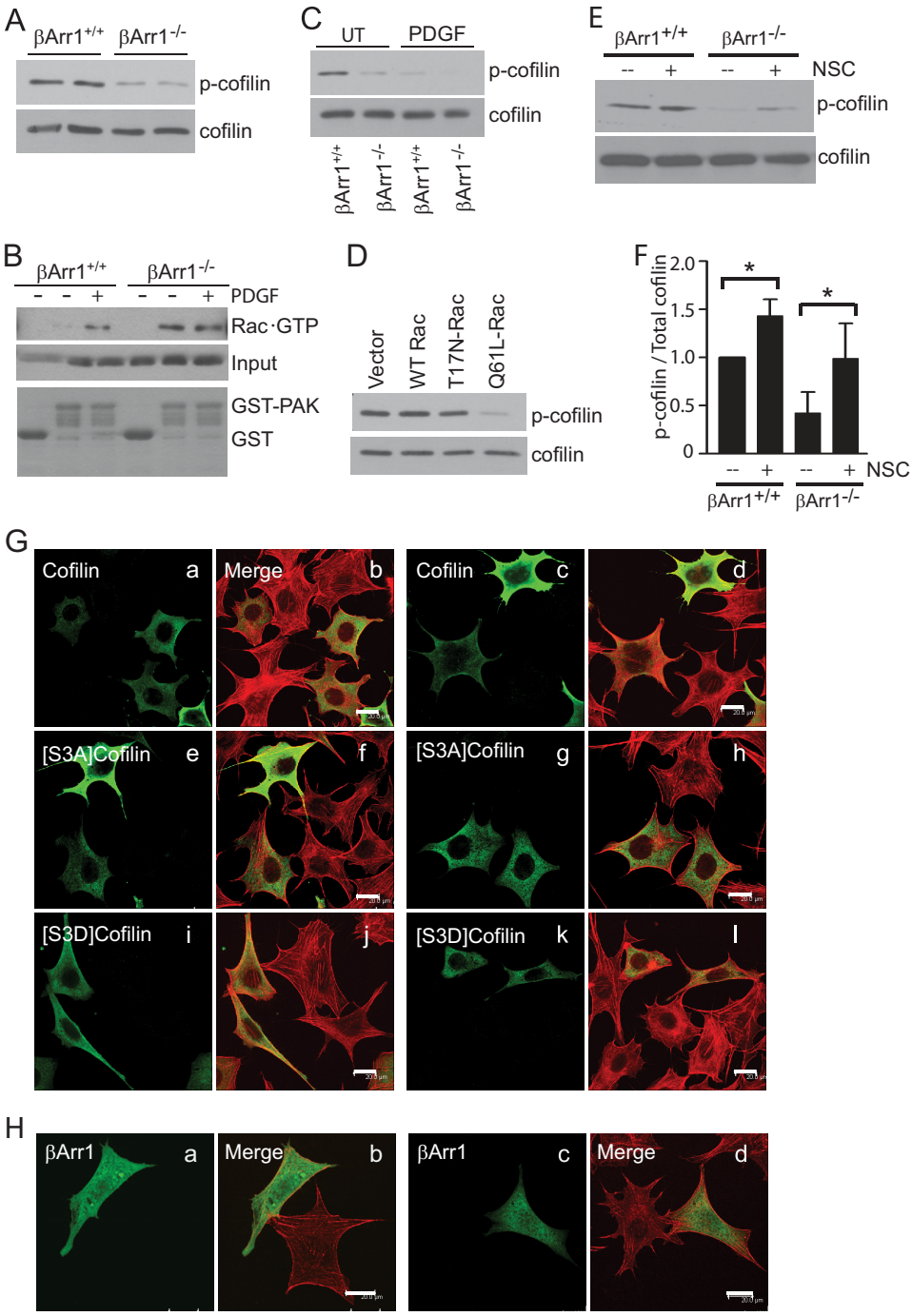


FIGURE 3. **βArr1 and Rac regulate cofilin phosphorylation.** *A,* cofilin dephosphorylation in $\beta Arr1^{-/-}$ MEFs. $\beta Arr1^{+/+}$ and $\beta Arr1^{-/-}$ MEFs were lysed, and cofilin phosphorylation was examined by Western blot, using total cofilin as a loading control. *B,* activation of Rac by PDGF. $\beta Arr1^{+/+}$ and $\beta Arr1^{-/-}$ MEFs were treated, or not, with PDGF (10 ng/ml) for 5 min, and active Rac levels were determined by pulldown. Total Rac was detected as a control (*middle panel*). *Bottom panel* shows staining of GST and GST-PAK used for the pulldown assay. *C,* PDGF-induced cofilin dephosphorylation. $\beta Arr1^{+/+}$ and $\beta Arr1^{-/-}$ MEFs were treated without (*UT*) or with PDGF (10 ng/ml, 5 min), and p-cofilin and total cofilin levels were determined by Western blots. *D,* active Rac-induced cofilin dephosphorylation. HEK293 cells were transfected with cDNAs encoding empty vector, wild-type Rac, (T17N)-Rac, or (Q61L)-Rac, and p-cofilin or total cofilin levels were determined by Western blot. *E,* Rac inhibition increases cofilin phosphorylation. $\beta Arr1^{+/+}$ and $\beta Arr1^{-/-}$ MEFs were treated with vehicle or NSC23766 (*NSC*) (50 $\mu$M, 48 h), and p-cofilin or total cofilin levels were determined by Western blot. *F,* relative cofilin phosphorylation in $\beta Arr1^{+/+}$ and $\beta Arr1^{-/-}$ MEFs as normalized to the level of total cofilin. *, $p < 0.05$ *versus* vehicle-treated. *G,* overexpression of (S3D)cofilin alters $\beta Arr1^{-/-}$ MEF morphology. Cells were transiently transfected with expression vectors encoding FLAG-tagged cofilin, (S3A)cofilin, or (S3D)cofilin for 48 h before morphology was examined by actin staining. Cofilin-expressing cells were identified by immunofluorescence staining with anti-FLAG antibody. *H,* restored expression of βArr1 alters $\beta Arr1^{-/-}$ MEF morphology. Cells were transiently transfected with empty vectors (data not shown) or expression vectors encoding HA-tagged βArr1. Cells were examined by staining with anti-HA antibody and rhodamine-conjugated phalloidin. *Scale bars,* 20 $\mu$m.

reduction of cofilin phosphorylation in $\beta Arr1^{-/-}$ MEFs compared with $\beta Arr1^{+/+}$ MEFs, implying a regulatory role for βArr1 on cofilin activity.

Cofilin is known to be activated by, among others, Rac (22). Higher activities for both Rac and cofilin in $\beta Arr1^{-/-}$ MEFs suggest that they function in the same pathway following βArr1

depletion to regulate actin polymerization. We compared the effects of platelet-derived growth factor (PDGF) on cofilin dephosphorylation in $\beta Arr1^{+/+}$ and $\beta Arr1^{-/-}$ MEFs. Treatment with PDGF significantly increased Rac activity in $\beta Arr1^{+/+}$ MEFs, and in $\beta Arr1^{-/-}$ MEFs whose basal Rac activity is high, PDGF stimulation failed to further increase the Rac activation (Fig. 3*B*). The similar treatment with PDGF resulted in cofilin dephosphorylation in $\beta Arr1^{+/+}$ MEFs (Fig. 3*C*). In $\beta Arr1^{-/-}$ MEFs whose basal cofilin phosphorylation level is low, PDGF stimulation only slightly augmented the dephosphorylation signal (Fig. 3*C*). To further implicate Rac in cofilin phosphorylation, we transfected HEK293 cells with cDNAs encoding (WT)Rac, (T17N)Rac, or (Q61L)Rac (to overcome the low transfection efficiency of MEFs). Expression of constitutively active (Q61L)Rac resulted in dephosphorylation of cofilin in unstimulated cells, whereas no difference in cofilin dephosphorylation was observed in cells overexpressing (WT)Rac or (T17N)Rac (Fig. 3*D*). These results suggest that cofilin serves as a Rac effector.

To test the possibility that elevated Rac activity contributes to the lowered phosphorylation level of cofilin in $\beta Arr1^{-/-}$ MEFs, we treated MEFs with NSC23766. Rac inhibition slightly increased the cofilin phosphorylation signal in $\beta Arr1^{+/+}$ MEFs (Fig. 3, *E* and *F*) and elevated cofilin phosphorylation level in $\beta Arr1^{-/-}$ MEFs to that of untreated $\beta Arr1^{+/+}$ MEFs (Fig. 3, *E* and *F*). These results link the higher Rac activity to increased cofilin activity in $\beta Arr1^{-/-}$ MEFs.

We next examined whether elevated cofilin activity contributes to the morphological characteristics of $\beta Arr1^{-/-}$ MEFs by overexpressing FLAG-tagged WT or mutated forms of cofilin. Expression of (WT)cofilin (Fig. 3*G*, *panels a–d*) or constitutively active (S3A)cofilin (Fig. 3*G*, *panels e–h*) did not affect morphology of $\beta Arr1^{-/-}$ MEFs, as determined by staining of actin. However, expression of dominant negative (S3D)cofilin changed $\beta Arr1^{-/-}$ MEFs from rounded with multiple protrusions to elongated with fewer protrusions (Fig. 3*G*, *panels i–l*).

To further support the idea that morphological characteristics of $\beta Arr1^{-/-}$ MEFs are a direct result of βArr1 loss of expression, we restored βArr1 protein expression in $\beta Arr1^{-/-}$ MEFs by transient transfection with HA-tagged βArr1. Overexpression of βArr1 altered morphology of $\beta Arr1^{-/-}$ MEFs, which were now more elongated with fewer protrusions (Fig. 3*H*, *panels a–d*). In contrast, overexpression of βArr1 protein did not affect morphology of $\beta Arr1^{+/+}$ MEFs (data not shown). These data suggest that loss of βArr1 expression results in higher Rac activity that functions, at least in part, through cofilin to regulate the cell morphology.

*Depletion of βArr1 Yields Higher rasgrf2 Gene Expression*—Elevated Rac activity in $\beta Arr1^{-/-}$ MEFs suggests that depletion of βArr1 activates Rac GEFs or inactivates RacGAPs. We used a SMARTpool siRNA library that targets known Rac GEFs to screen for changes in membrane protrusion and circularity of $\beta Arr1^{-/-}$ MEFs. Among the 23 Rac GEFs examined, knockdown of Tiam1, ARHGEF6, RasGRF2, and DOCK4 reduced protrusion numbers (Fig. 4*A*) and, concordantly, promoted elongation of the $\beta Arr1^{-/-}$ MEFs (Fig. 4*B*) as determined by decreased cell circularity. Next, we performed real time PCR to examine whether gene levels of these four Rac GEFs were up-regulated in $\beta Arr1^{-/-}$ MEFs. Results show that mRNA levels of *tiam1* and *arhgef6* were lower in $\beta Arr1^{-/-}$ than in $\beta Arr1^{+/+}$ MEFs (Fig. 4*C*). However, *dock4* mRNA levels were about four times higher, and *rasgrf2* mRNA levels were 120 times higher in $\beta Arr1^{-/-}$ compared with $\beta Arr1^{+/+}$ MEFs (Fig. 4*C*). Because *rasgrf2* levels were the most changed among the $\beta Arr1^{+/+}$ and $\beta Arr1^{-/-}$ MEFs, we examined the RasGRF2 protein level and consistently observed it to be higher in $\beta Arr1^{-/-}$ than in $\beta Arr1^{+/+}$ MEFs (Fig. 4*D*). To rule out the possibility of cell type-specific effects, we measured RasGRF2 protein expression in human kidney cancer RCC7 cells with transient knockdown of βArr1. Western blot results showed that RasGRF2 protein was hardly detectable in control RCC7 cells, and knockdown of βArr1 significantly increased the RasGRF2 levels (Fig. 4*E*). Mirroring our observations with $\beta Arr1^{-/-}$ MEFs (Fig. 3), the knockdown of βArr1 in RCC7 cells also resulted in cofilin activation as reflected by its dephosphorylation (Fig. 4*E*).

*βArr1 Regulates Cofilin Activity through RasGRF2*—RasGRF2 is a dual exchange factor for both Rac and Ras, and therefore, the elevated expression of RasGRF2 may increase Ras activity, which promotes ERK phosphorylation. Basal ERK phosphorylation appeared higher in $\beta Arr1^{-/-}$ than in $\beta Arr1^{+/+}$ MEFs (Fig. 5*A*), consistent with the idea that higher RasGRF2 expression associates with concomitantly higher Ras activity. PDGF treatment elicited strong ERK phosphorylation that was slightly higher in $\beta Arr1^{-/-}$ than in $\beta Arr1^{+/+}$ MEFs (Fig. 5*A*).

We examined whether activation of Ras is required for dephosphorylation and activation of cofilin. To this end, we overexpressed the empty vector, FLAG-RasGRF2 (which activates both Ras and Rac) or FLAG-ΔCdc25-RasGRF2 (which activates Rac only), and determined cofilin phosphorylation. As shown in Fig. 5*B*, both FLAG-RasGRF2 and FLAG-ΔCdc25-RasGRF2 were expressed to similar levels. In cells with overexpression of either protein, the level of cofilin phosphorylation was lower than that in control empty vector-transfected cells (Fig. 5*B*). To ascertain that the overexpressed ΔCdc25-RasGRF2 is functional, we performed pulldown assays to measure active Rac. Western blot results indicated that overexpression of GFP-ΔCdc25-RasGRF2 increased Rac·GTP levels by an average 3-fold (Fig. 5*C*). These results suggest that elevated Rac activity is sufficient to activate cofilin in $\beta Arr1^{-/-}$ MEFs.

We asked if RasGRF2 is necessary for cofilin activation in $\beta Arr1^{-/-}$ MEFs. Knockdown of endogenous RasGRF2 expression in $\beta Arr1^{+/+}$ and $\beta Arr1^{-/-}$ MEFs was achieved using siRNA and confirmed at the gene level by RT-PCR (Fig. 5*D*) and the protein level by Western blot (Fig. 5*E*). We next examined whether RasGRF2 knockdown would affect Rac activity using pulldown assays. Suppression of RasGRF2 expression lowered active Rac levels in $\beta Arr1^{-/-}$ MEFs by about 2-fold. We then examined whether suppression of RasGRF2 expression affected cofilin phosphorylation. Western blot results indicated that the knockdown of RasGRF2 did not impact total cofilin expression in $\beta Arr1^{+/+}$ MEFs (Fig. 5, *F* and *G*). However, the knockdown of RasGRF2 significantly increased cofilin phosphorylation levels in $\beta Arr1^{-/-}$ MEFs (Fig. 5, *F* and *G*), suggesting that RasGRF2 is a required component for cofilin activation following depletion of βArr1.

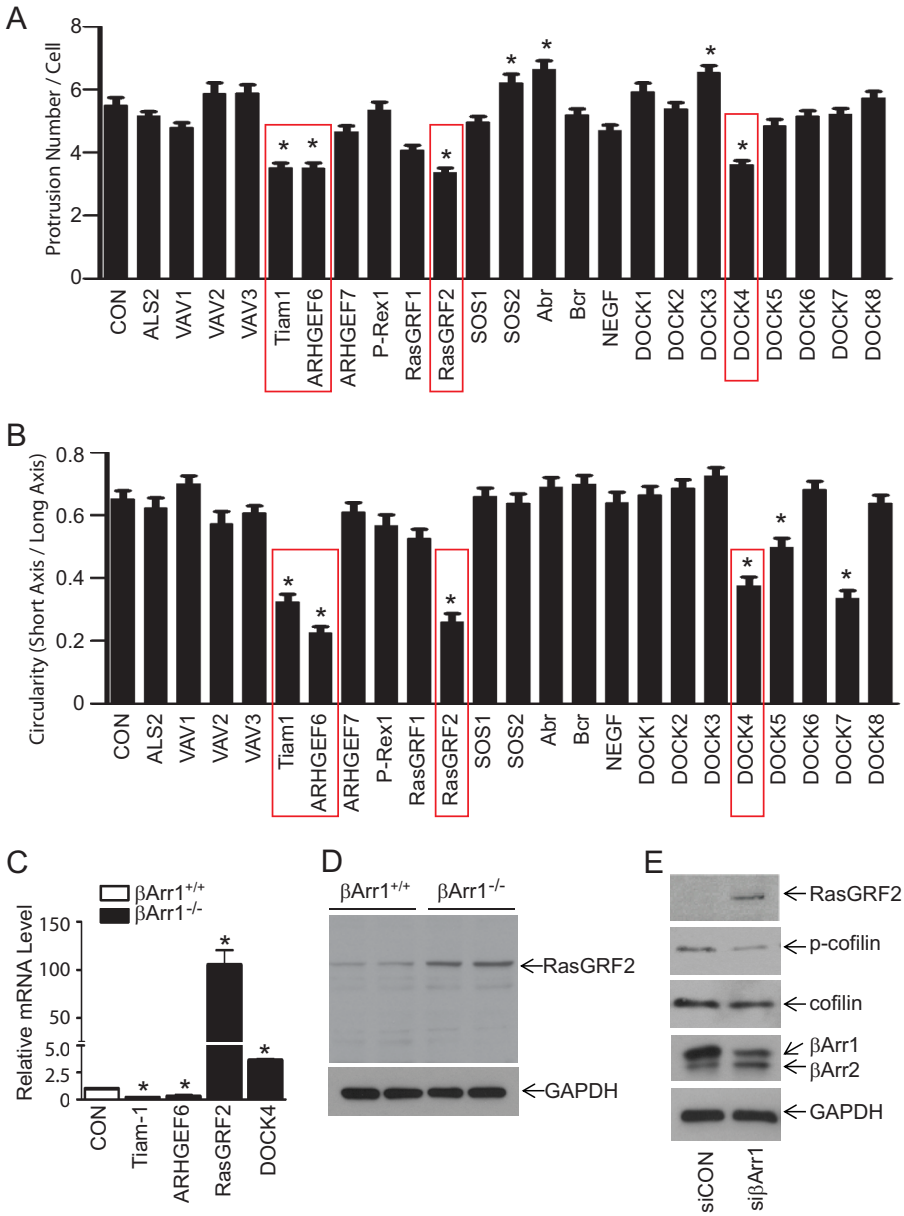


FIGURE 4. **Depletion of βArr1 increases transcriptional expression of *rasgrf2*.** *A,* blockade of multipolar protrusion formation in $\beta Arr1^{-/-}$ MEFs following knockdown of select Rac GEFs by siRNA. *, $p < 0.05$ *versus* siRNA control (*CON*). *Error bars* represent mean ± S.E. Quantification was made from two coverslips with more than 130 cells counted in each group. *B,* blockade of increased circularity of $\beta Arr1^{-/-}$ MEFs following knockdown of select Rac GEFs by siRNA. *, $p < 0.05$ *versus* control. Quantification was made from two coverslips with more than 130 cells counted in each group. *C,* relative mRNA levels of four select Rac GEFs were determined by real time PCR, and the values are expressed relative to the corresponding levels in $\beta Arr1^{+/+}$ MEFs. *, $p < 0.05$ *versus* $\beta Arr1^{+/+}$ control MEFs. *D,* RasGRF2 protein expression in $\beta Arr1^{+/+}$ and $\beta Arr1^{-/-}$ MEFs. MEFs were lysed and RasGRF2 protein levels examined by Western blot. GAPDH was detected as a loading control. *E,* transient knockdown of βArr1 increased RasGRF2 protein expression. RCC7 cells were transfected with control or βArr1 siRNA. Western blot was performed to examine the expression of RasGRF2, cofilin, p-cofilin, βArr1 and βArr2, and GAPDH.

To provide direct evidence that up-regulated RasGRF2 expression is critical for the morphological properties of βArr1 MEFs, we examined the effect of RasGRF2 knockdown. Control siRNA-transfected $\beta Arr1^{-/-}$ MEFs appeared round with multiple protrusions (Fig. 5*H*, *panels a* and *b*), whereas $\beta Arr1^{-/-}$ MEFs with RasGRF2 knockdown became elongated with fewer protrusions (Fig. 5*H*, *panels c* and *d*). These data support that Rac and cofilin regulate cell morphology of $\beta Arr1^{-/-}$ MEFs.

We performed chromatin immunoprecipitation (ChIP) to test whether βArr1 bound to the promoter region of the *rasgrf2* gene. The binding of βArr1 to the p21 gene promoter has been reported (23), and we included the p21 promoter as a positive control (Fig. 6*A*). βArr1 bound to the *rasgrf2* promoter region, and the ChIP signal was much weaker in $\beta Arr1^{-/-}$ MEFs compared with $\beta Arr1^{+/+}$ MEFs (Fig. 6*A*). The *rasgrf2* promoter was reported to be heavily methylated in human cancer cells (24), and we examined whether promoter methylation contributed to the differential expression of the *rasgrf2* gene. We treated $\beta Arr1^{+/+}$ and $\beta Arr1^{-/-}$ MEFs with the demethylating agent decitabine (*i.e.* 5-aza-2′-deoxycytidine) and determined the *rasgrf2* mRNA levels using real time PCR. Basal *rasgrf2* mRNA levels were higher in $\beta Arr1^{-/-}$ than in $\beta Arr1^{+/+}$ MEFs (Fig. 6*B*). Treatment with decitabine increased *rasgrf2* mRNA levels by about 400-fold (over corresponding untreated samples) in

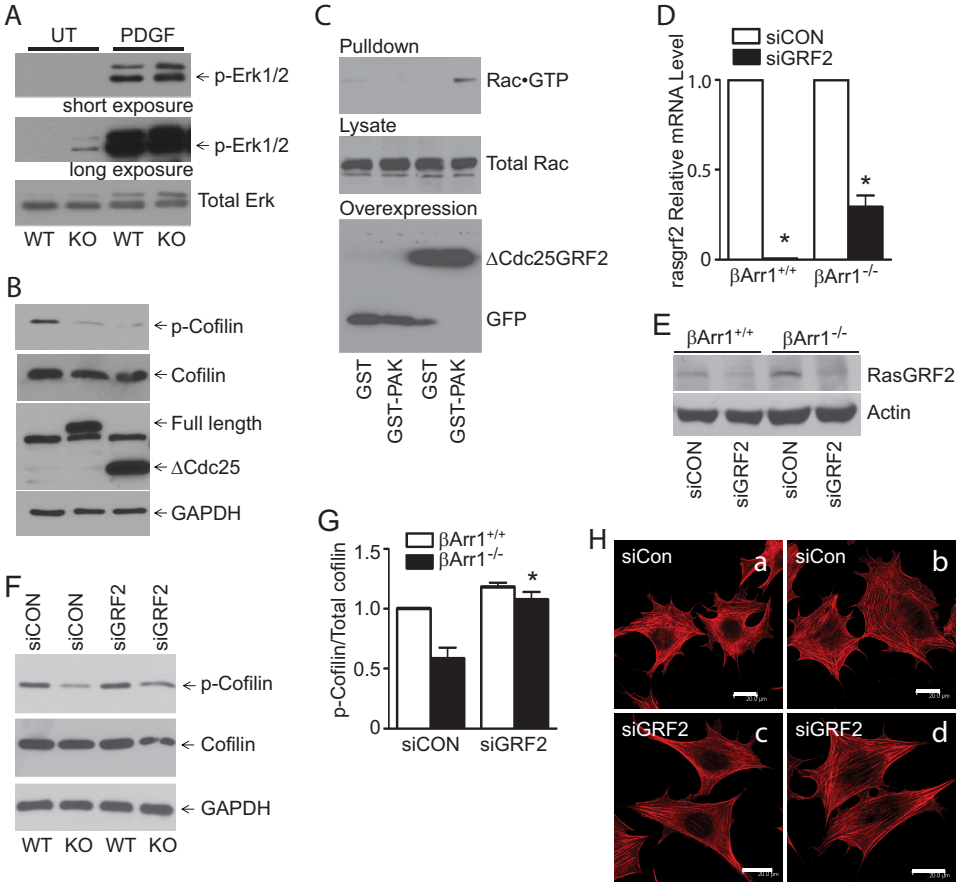


FIGURE 5. **βArr1 regulates cofilin phosphorylation through RasGRF2.** *A*, PDGF promotes ERK phosphorylation. $\beta Arr1^{+/+}$ (WT) and $\beta Arr1^{-/-}$ (KO) MEFs were treated with PDGF (10 ng/ml; 5 min), and cell lysates were subjected to ERK phosphorylation analysis by Western blot (*top* and *middle panels*). Total ERK was used as a protein loading control (*bottom panel*). *UT*, untreated. *B*, overexpression of RasGRF2 induced cofilin dephosphorylation. RCC7 cells were transfected with cDNAs encoding empty vector, FLAG-RasGRF2, or FLAG-ΔCdc25-RasGRF2. Western blot was performed to detect the expression of RasGRF2, and phosphorylation of cofilin, using total cofilin and GAPDH as loading controls. *C*, ΔCdc25RasGRF2 activates Rac. HEK293 cells were transiently transfected with vectors encoding GFP-ΔCdc25RasGRF2 or GFP alone, and cell lysates were used for pulldown with GST or GST-PAK to determine Rac·GTP level (*top panel*). *Middle panel* shows expression of total Rac, and *bottom panel* shows expression of GFP-ΔCdc25RasGRF2 or GFP as determined with Western blot. *D* and *E*, $\beta Arr1^{+/+}$ and $\beta Arr1^{-/-}$ MEFs were transfected with control or RasGRF2 siRNA, and knockdown efficiency was determined by real time PCR (*D*) and Western blot (*E*). *F*, effect of RasGRF2 knockdown on cofilin dephosphorylation. Western blot was performed to examine the p-cofilin, total cofilin, and GAPDH levels. *G*, level of p-cofilin was normalized to total cofilin. *, $p < 0.05$ *versus* siCON. *H*, knockdown of RasGRF2 alters $\beta Arr1^{-/-}$ MEF morphology. Cells were transfected with control (*panels a* and *b*) or RasGRF2 (*panels c* and *d*) targeting siRNA for 48 h, and morphology was examined by actin staining.

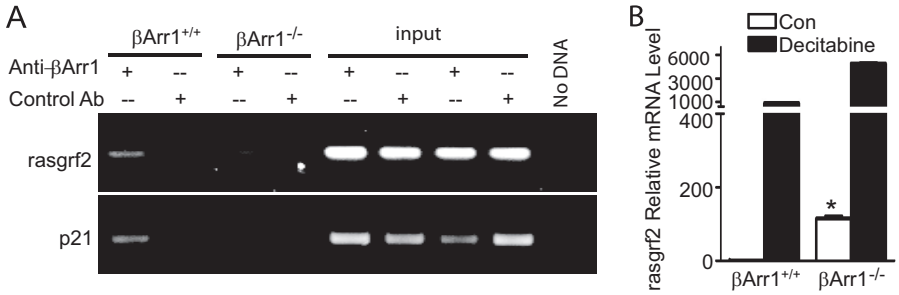


FIGURE 6. **βArr1 regulates *rasgrf2* gene expression.** *A*, βArr1 binds promoter region of *rasgrf2*. ChIP was performed to detect the binding between βArr1 protein and *rasgrf2* gene promoter, and βArr1 binding to p21 promoter region served as a positive control. *B*, effect of decitabine on *rasgrf2* gene expression. $\beta Arr1^{+/+}$ and $\beta Arr1^{-/-}$ MEFs were treated with decitabine (1 μM) on 3 alternate days for a total of 6 days. *, $p < 0.05$ *versus* $\beta Arr1^{+/+}$ MEFs.

both $\beta Arr1^{+/+}$ and $\beta Arr1^{-/-}$ MEFs (Fig. 6*B*). These results suggest that βArr1 regulates *rasgrf2* gene expression, at least in part, through promoter DNA methylation.

*βArr1 Regulates RCC Cell Migration and Invasion*—Actin polymerization is crucial for formation of polarized protrusions that are required for the directional cell migration and invasion. We examined the effect of βArr1 knockdown on the migration of several RCC cell lines using Transwells. The results revealed that knockdown of βArr1 dramatically decreased directional migration of Caki-1 (Fig. 7*A*) and RCC7 (data not shown) cells. As migration constitutes a critical step of cell invasion, we examined the effects of βArr1 knockdown on the cell invasion through a Matrigel matrix. Suppression of βArr1 expression with siRNA significantly reduced invasion of RCC7 (Fig. 7*B*)

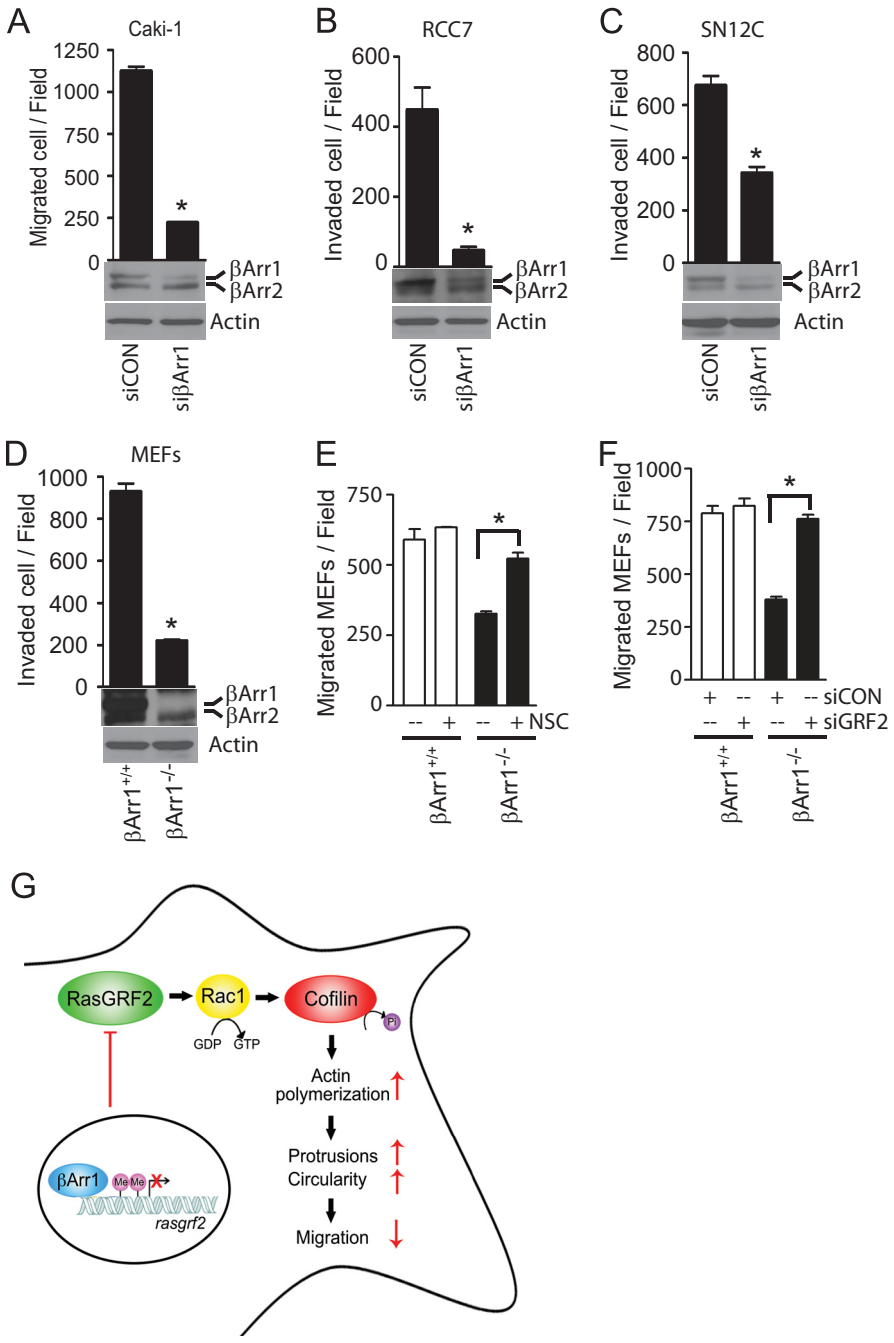


FIGURE 7. **βArr1 regulates cell migration and invasion through Rac.** *A–C,* βArr1 was required for RCC cell migration and invasion. Transient knockdown of βArr1 expression was performed using siRNA in Caki-1, RCC7, and SN12C cells and verified by Western blot, using actin as a loading control (*lower panels* below the *bar graphs*). Caki-1 cell migration was examined using Boyden chamber (*A*) and RCC7 (*B*), and SN12C (*C*) cell invasion was examined using Matrigel-coated filters. *, $p < 0.05$ *versus* siCON. *D,* deletion of βArr1 inhibited MEF invasion. $\beta Arr1^{+/+}$ and $\beta Arr1^{-/-}$ MEFs were used for the cell invasion, and expression of βArr1 was examined by Western blot using actin as a loading control (*lower panels*). *, $p < 0.05$ *versus* $\beta Arr1^{+/+}$ MEFs. *E,* inhibition of Rac activity increases migration rate of $\beta Arr1^{-/-}$ MEFs. $\beta Arr1^{+/+}$ and $\beta Arr1^{-/-}$ MEFs were treated with NSC23766 (*NSC*) (50 μM) for 48 h, and migration toward a gradient of FBS was examined using Transwells. *, $p < 0.05$ *versus* untreated samples. *F,* knockdown of rasGRF2 increases migration rate of $\beta Arr1^{-/-}$ MEFs. $\beta Arr1^{+/+}$ and $\beta Arr1^{-/-}$ MEFs were transfected with control or RasGRF2 siRNA, and cell migration was examined using Transwells. *, $p < 0.05$ *versus* control. *G,* schematic diagram of βArr1-mediated inhibition of *rasgrf2* gene expression. RasGrf2, a dual Ras/Rac guanine nucleotide exchange factor, activates Rac to promote actin polymerization through dephosphorylation and activation of cofilin. This leads to the formation of multiple protrusions and increased circularity of cells with a consequent decrease of directional cell migration. In the nucleus, βArr1 inhibits the gene expression of *rasgrf2* through, at least in part, enhanced methylation of the promoter region. Suppression of βArr1 expression results in higher RasGRF2 and Rac activity.

and SN12C (Fig. 7*C*) cells. A similar effect was observed using βArr1 knock-out MEFs, *i.e.* $\beta Arr1^{+/+}$ MEFs invaded through Matrigel more efficiently than $\beta Arr1^{-/-}$ MEFs (Fig. 7*D*).

Next, we examined whether higher Rac activity contributes to the reduced cell migration following depletion of βArr1 expression. Inhibition of Rac activity with NSC23766 did not affect migration of $\beta Arr1^{+/+}$ MEFs (Fig. 7*E*). Distinctly, the inhibition of Rac activity increased the migration of $\beta Arr1^{-/-}$ MEFs (Fig. 7*E*). These results suggest that deregulated high Rac activity contributes to the lowered rate of directional migration

of βArr1$^{-/-}$ MEFs. As our results suggest that higher Rac activity in βArr1$^{-/-}$ MEFs resulted from the up-regulated expression of RasGRF2, we examined possible effects of RasGRF2 knockdown. Suppression of RasGRF2 expression with siRNA did not impact migration of βArr1$^{+/+}$ MEFs (Fig. 7*F*) but increased the migration rate of βArr1$^{-/-}$ MEFs (Fig. 7*F*), consistent with the idea that increased expression of RasGRF2 leads to deregulated Rac activity that, in turn, contributes to the lowered cell migration.

## DISCUSSION

βArrs control GPCR signaling through receptor desensitization and down-regulation, as well as perturbation of the second messenger level (25). In addition, βArrs function as scaffolds to transduce signals from GPCRs, and the best described examples include activation of c-Src and ERK (6). Because of the absence of nuclear export signal, βArr1 is also present in the nucleus (26), where it can regulate gene transcription. Indeed, βArr1 was shown to increase the transcription of IL-1β (27), p27, and c-*fos* (28) genes. βArr1 was also shown to negatively regulate transcription of γ-interferon-responsive genes (29). Here, we observed inhibition of *rasgrf2* gene expression by βArr1; depletion of βArr1 resulted in the up-regulation of *rasgrf2* mRNA and protein levels. The results also show that βArr1 binds to the promoter region of *rasgrf2* gene, and treatment with the demethylating agent decitabine significantly increased *rasgrf2* gene expression. Together, these results suggest that βArr1 regulates cell morphology and migration through RasGRF2-related mechanisms.

The *rasgrf2* gene was reported to be aberrantly methylated in the CpG island at the 5′ region in human pancreatic cancer cells, and treatment with decitabine restored *rasgrf2* gene expression (24). Similarly, reduced *rasgrf2* gene or protein expression was observed in mammary carcinoma tissues (30), in non-small cell lung cancers (31), and in benign colorectal adenoma as well as invasive colon carcinomas (32). Restoration of RasGRF2 expression resulted in a 56% reduction of colony formation of the colorectal cancer cell line HCT-116 (32), and deletion of RasGRF2 accelerated development of lymphoblastic lymphoma-like tumors in mice (33), suggesting a tumor-suppressive role for RasGRF2. A recent study showed that βArr1 functions as an E3 ligase adaptor in the nucleus to mediate p53 degradation and accumulation of DNA damage in response to chronic stress (23). Hence, nuclear βArr1 can either suppress the expression or facilitate the degradation of tumor suppressors, which may contribute to human tumor initiation and progression.

RasGRF2 promotes exchange activities on both Ras and Rac GTPases (34); activation of either pathway can have profound effects on actin remodeling and cancer cell migration (35). A recent study showed that RasGRF2 regulates cancer cell invasion through direct binding to Cdc42 thereby sequestering it from association with cognate GEFs, and knockdown of RasGRF2 increased rounded invasion of melanoma cells (36). Here, we observed activation of Rac by RasGRF2 following depletion of βArr1. It is not clear at present how RasGRF2 activates Rac in MEFs and RCC cell lines yet inhibits Cdc42 activation in melanoma cells (36).

Rac is known to promote actin polymerization at cell protrusions through the activation of, among others, the actin-severing protein cofilin (37) whose activity is tightly controlled by phosphorylation (38). Phosphorylation of serine 3 by LIM kinase inhibits cofilin binding to actin, and dephosphorylation of cofilin by slingshot or chronophin activates it (38). Our results show that depletion of βArr1 results in cofilin dephosphorylation, which is a direct effect of up-regulated expression of RasGRF2 and consequent activation of Rac. This effect can be mimicked by overexpression of RasGRF2 or constitutively active Rac and, concordantly, the knockdown of RasGRF2 in βArr1$^{-/-}$ MEFs reversed this effect. As shown in Fig. 7*G*, we propose a model where βArr1 suppresses *rasgrf2* gene expression through, at least in part, enhanced methylation of the promoter region. Knock-out of βArr1 results in higher RasGRF2 and Rac activity. Treatment with the demethylation agent decitabine increased *rasgrf2* gene expression in βArr1 knockout cells. Decitabine also increased rasgrf2 expression level in wild-type cells, implying additional factors are involved in the methylation of rasgrf2 gene promoter. It can be envisioned that activated Rac leads to activation of slingshot family phosphatase to dephosphorylate and activate cofilin, as has been reported for keratinocyte migration (39). It is also worth mentioning that Rac was reported to inactivate cofilin through LIM kinase-mediated phosphorylation (40, 41). Therefore, additional regulatory mechanisms are likely involved in the fine-tuning of cofilin activity.

βArr2 was reported to function as a scaffold for cofilin and the phosphatases slingshot and chronophin in HEK293, leukocytes, and breast cancer cells (42–44). This multiprotein complex formation facilitated cofilin dephosphorylation, actin polymerization, and protrusion formation. Depletion of βArr2 resulted in cell migration defects (43). Here, we showed that βArr1 regulates *rasgrf2* expression at the transcription level with a consequent effect on Rac and cofilin activities and cell migration. Therefore, βArr1 and βArr2 may function coordinately at the transcriptional and post-translational levels to regulate cofilin activity, actin remodeling, and cell migration.

In summary, our results show that βArr1 suppressed *rasgrf2* gene expression presumably through promoter hypermethylation. Depletion of βArr1 resulted in up-regulated expression of RasGRF2 with consequent activation of Rac and cofilin and concomitant formation of multipolar protrusions and cell rounding, leading to reduced cell migration and invasion. Inhibitory effects on cell migration and invasion may contribute to the putative tumor-suppressive role for RasGRF2, and expression or function of nuclear βArr1 may be targeted to restore expression of RasGRF2 for human cancer therapy.

*Acknowledgments—We thank Dr. R. J. Lefkowitz for providing the βArr1 WT and KO MEFs and A1CT anti-βarrestin antibody; Dr. W. J. Koch for βArr1-expressing adenoviruses; Dr. P. Crespo for full-length and ΔCdc25 RasGRF2 cDNAs; and Dr. C. Smith for WT and mutant cofilin cDNAs. We also thank Dr. C. Moneypenny for help with live cell imaging, and J. Patel for technical assistance.*

## REFERENCES


1. Ridley, A. J., Schwartz, M. A., Burridge, K., Firtel, R. A., Ginsberg, M. H., Borisy, G., Parsons, J. T., and Horwitz, A. R. (2003) Cell migration: integrating signals from front to back. *Science* **302,** 1704–1709
2. Rossman, K. L., Der, C. J., and Sondek, J. (2005) GEF means go: turning on Rho GTPases with guanine nucleotide-exchange factors. *Nat. Rev. Mol. Cell Biol.* **6,** 167–180
3. Côté, J. F., and Vuori, K. (2007) GEF what? Dock 180 and related proteins help Rac to polarize cells in new ways. *Trends Cell Biol.* **17,** 383–393
4. Fernández-Medarde, A., and Santos, E. (2011) The RasGRF family of mammalian guanine nucleotide exchange factors. *Biochim. Biophys. Acta* **1815,** 170–188
5. Feig, L. A. (2011) Regulation of neuronal function by RasGRF exchange factors. *Genes Cancer* **2,** 306–319
6. Shukla, A. K., Xiao, K., and Lefkowitz, R. J. (2011) Emerging paradigms of βarrestin-dependent seven transmembrane receptor signaling. *Trends Biochem. Sci.* **36,** 457–469
7. Kim, J. I., Lakshmikanthan, V., Frilot, N., and Daaka, Y. (2010) Prostaglandin E2 promotes lung cancer cell migration via EP4-βArrestin1-c-Src signalsome. *Mol. Cancer Res.* **8,** 569–577
8. Lakshmikanthan, V., Zou, L., Kim, J. I., Michal, A., Nie, Z., Messias, N. C., Benovic, J. L., and Daaka, Y. (2009) Identification of βarrestin2 as a corepressor of androgen receptor signaling in prostate cancer. *Proc. Natl. Acad. Sci. U.S.A.* **106,** 9379–9384
9. Michal, A. M., Peck, A. R., Tran, T. H., Liu, C., Rimm, D. L., Rui, H., and Benovic, J. L. (2011) Differential expression of arrestins is a predictor of breast cancer progression and survival. *Breast Cancer Res. Treat.* **130,** 791–807
10. Fereshteh, M., Ito, T., Kovacs, J. J., Zhao, C., Kwon, H. Y., Tornini, V., Konuma, T., Chen, M., Lefkowitz, R. J., and Reya, T. (2012) βArrestin2 mediates the initiation and progression of myeloid leukemia. *Proc. Natl. Acad. Sci. U.S.A.* **109,** 12532–12537
11. DeFea, K. A. (2007) Stop that cell! βArrestin-dependent chemotaxis: a tale of localized actin assembly and receptor desensitization. *Annu. Rev. Physiol.* **69,** 535–560
12. Cotton, M., and Claing, A. (2009) G protein-coupled receptors stimulation and the control of cell migration. *Cell. Signal.* **21,** 1045–1053
13. Barnes, W. G., Reiter, E., Violin, J. D., Ren, X. R., Milligan, G., and Lefkowitz, R. J. (2005) βArrestin1 and Gqα/11 coordinately activate RhoA and stress fiber formation following receptor stimulation. *J. Biol. Chem.* **280,** 8041–8050
14. Mythreye, K., and Blobe, G. C. (2009) The type III TGFβ receptor regulates directional migration: new tricks for an old dog. *Cell Cycle* **8,** 3069–3070
15. Li, T. T., Alemayehu, M., Aziziyeh, A. I., Pape, C., Pampillo, M., Postovit, L. M., Mills, G. B., Babwah, A. V., and Bhattacharya, M. (2009) βArrestin/Ral signaling regulates lysophosphatidic acid-mediated migration and invasion of human breast tumor cells. *Mol. Cancer Res.* **7,** 1064–1077
16. Anthony, D. F., Sin, Y. Y., Vadrevu, S., Advant, N., Day, J. P., Byrne, A. M., Lynch, M. J., Milligan, G., Houslay, M. D., and Baillie, G. S. (2011) βArrestin1 inhibits the GTPase-activating protein function of ARHGAP21, promoting activation of RhoA following angiotensin II type 1A receptor stimulation. *Mol. Cell. Biol.* **31,** 1066–1075
17. Guilluy, C., Brégeon, J., Toumaniantz, G., Rolli-Derkinderen, M., Retailleau, K., Loufrani, L., Henrion, D., Scalbert, E., Bril, A., Torres, R. M., Offermanns, S., Pacaud, P., and Loirand, G. (2010) The Rho exchange factor Arhgef1 mediates the effects of angiotensin II on vascular tone and blood pressure. *Nat. Med.* **16,** 183–190
18. Ma, X., Zhao, Y., Daaka, Y., and Nie, Z. (2012) Acute activation of β2-adrenergic receptor regulates focal adhesions through βarrestin2- and p115RhoGEF protein-mediated activation of RhoA. *J. Biol. Chem.* **287,** 18925–18936
19. Cernuda-Morollon, E., Millan, J., Shipman, M., Marelli-Berg, F. M., and Ridley, A. J. (2010) Rac activation by the T-cell receptor inhibits T cell migration. *PLoS One* **5,** e12393
20. Moniri, N. H., and Daaka, Y. (2007) Agonist-stimulated reactive oxygen species formation regulates β2-adrenergic receptor signal transduction. *Biochem. Pharmacol.* **74,** 64–73
21. Gao, Y., Dickerson, J. B., Guo, F., Zheng, J., and Zheng, Y. (2004) Rational design and characterization of a Rac GTPase-specific small molecule inhibitor. *Proc. Natl. Acad. Sci. U.S.A.* **101,** 7618–7623
22. Pandey, D., Goyal, P., Dwivedi, S., and Siess, W. (2009) Unraveling a novel Rac1-mediated signaling pathway that regulates cofilin dephosphorylation and secretion in thrombin-stimulated platelets. *Blood* **114,** 415–424
23. Hara, M. R., Kovacs, J. J., Whalen, E. J., Rajagopal, S., Strachan, R. T., Grant, W., Towers, A. J., Williams, B., Lam, C. M., Xiao, K., Shenoy, S. K., Gregory, S. G., Ahn, S., Duckett, D. R., and Lefkowitz, R. J. (2011) A stress response pathway regulates DNA damage through β2-adrenoreceptors and βarrestin1. *Nature* **477,** 349–353
24. Hagihara, A., Miyamoto, K., Furuta, J., Hiraoka, N., Wakazono, K., Seki, S., Fukushima, S., Tsao, M. S., Sugimura, T., and Ushijima, T. (2004) Identification of 27 5′ CpG islands aberrantly methylated and 13 genes silenced in human pancreatic cancers. *Oncogene* **23,** 8705–8710
25. Shenoy, S. K., and Lefkowitz, R. J. (2011) βArrestin-mediated receptor trafficking and signal transduction. *Trends Pharmacol. Sci.* **32,** 521–533
26. Scott, M. G., Le Rouzic, E., Périanin, A., Pierotti, V., Enslen, H., Benichou, S., Marullo, S., and Benmerah, A. (2002) Differential nucleocytoplasmic shuttling of βarrestins: characterization of a leucine-rich nuclear export signal in βarrestin2. *J. Biol. Chem.* **277,** 37693–37701
27. Hoeppner, C. Z., Cheng, N., and Ye, R. D. (2012) Identification of a nuclear localization sequence in βarrestin1 and its functional implications. *J. Biol. Chem.* **287,** 8932–8943
28. Kang, J., Shi, Y., Xiang, B., Qu, B., Su, W., Zhu, M., Zhang, M., Bao, G., Wang, F., Zhang, X., Yang, R., Fan, F., Chen, X., Pei, G., and Ma, L. (2005) A nuclear function of βarrestin1 in GPCR signaling: regulation of histone acetylation and gene transcription. *Cell* **123,** 833–847
29. Mo, W., Zhang, L., Yang, G., Zhai, J., Hu, Z., Chen, Y., Chen, X., Hui, L., Huang, R., and Hu, G. (2008) Nuclear βarrestin1 functions as a scaffold for the dephosphorylation of STAT1 and moderates the antiviral activity of IFNγ. *Mol. Cell* **31,** 695–707
30. Qiu, C., Yu, M., Shan, L., and Snyderwine, E. G. (2003) Allelic imbalance and altered expression of genes in chromosome 2q11–2q16 from rat mammary gland carcinomas induced by 2-amino-1-methyl-6-phenylimidazo 4,5-*b* pyridine. *Oncogene* **22,** 1253–1260
31. Chen, H., Suzuki, M., Nakamura, Y., Ohira, M., Ando, S., Iida, T., Nakajima, T., Nakagawara, A., and Kimura, H. (2006) Aberrant methylation of RasGRF2 and RasSF1A in human non-small cell lung cancer. *Oncol. Rep.* **15,** 1281–1285
32. Jacinto, F. V., Ballestar, E., Ropero, S., and Esteller, M. (2007) Discovery of epigenetically silenced genes by methylated DNA immunoprecipitation in colon cancer cells. *Cancer Res.* **67,** 11481–11486
33. Ruiz, S., Santos, E., and Bustelo, X. R. (2009) The use of knockout mice reveals a synergistic role of the Vav1 and RasGRF2 gene deficiencies in lymphomagenesis and metastasis. *PLoS One* **4,** 8229
34. Fan, W. T., Koch, C. A., de Hoog, C. L., Fam, N. P., and Moran, M. F. (1998) The exchange factor RasGRF2 activates Ras-dependent and Rac-dependent mitogen-activated protein kinase pathways. *Curr. Biol.* **8,** 935–938
35. Charest, P. G., and Firtel, R. A. (2007) Big roles for small GTPases in the control of directed cell movement. *Biochem. J.* **401,** 377–390
36. Calvo, F., Sanz-Moreno, V., Agudo-Ibáñez, L., Wallberg, F., Sahai, E., Marshall, C. J., and Crespo, P. (2011) RasGRF suppresses Cdc42-mediated tumor cell movement, cytoskeletal dynamics and transformation. *Nat. Cell Biol.* **13,** 819–926
37. Bernstein, B. W., and Bamburg, J. R. (2010) ADF/Cofilin: a functional node in cell biology. *Trends Cell Biol.* **20,** 187–195
38. Oser, M., and Condeelis, J. (2009) The cofilin activity cycle in lamellipodia and invadopodia. *J. Cell Biochem.* **108,** 1252–1262
39. Kligys, K., Claiborne, J. N., DeBiase, P. J., Hopkinson, S. B., Wu, Y., Mizuno, K., and Jones, J. C. (2007) The slingshot family of phosphatases mediates Rac1 regulation of cofilin phosphorylation, laminin-332 organization, and motility behavior of keratinocytes. *J. Biol. Chem.* **282,** 32520–32528
40. Yang, N., Higuchi, O., Ohashi, K., Nagata, K., Wada, A., Kangawa, K., Nishida, E., and Mizuno, K. (1998) Cofilin phosphorylation by LIM-kinase 1 and its role in Rac-mediated actin reorganization. *Nature* **393,** 809–812

41. Edwards, D. C., Sanders, L. C., Bokoch, G. M., and Gill, G. N. (1999) Activation of LIM-kinase by Pak1 couples Rac/Cdc42 GTPase signalling to actin cytoskeletal dynamics. *Nat. Cell Biol.* **1,** 253–259
42. Zoudilova, M., Kumar, P., Ge, L., Wang, P., Bokoch, G. M., and DeFea, K. A. (2007) βArrestin-dependent regulation of the cofilin pathway downstream of protease-activated receptor-2. *J. Biol. Chem.* **282,** 20634–20646
43. Zoudilova, M., Min, J., Richards, H. L., Carter, D., Huang, T., and DeFea, K. A. (2010) βArrestins scaffold cofilin with chronophin to direct localized actin filament severing and membrane protrusions downstream of protease-activated receptor-2. *J. Biol. Chem.* **285,** 14318–14329
44. Xiao, K., Sun, J., Kim, J., Rajagopal, S., Zhai, B., Villén, J., Haas, W., Kovacs, J. J., Shukla, A. K., Hara, M. R., Hernandez, M., Lachmann, A., Zhao, S., Lin, Y., Cheng, Y., Mizuno, K., Ma'ayan, A., Gygi, S. P., and Lefkowitz, R. J. (2010) Global phosphorylation analysis of βarrestin-mediated signaling downstream of a seven transmembrane receptor. *Proc. Natl. Acad. Sci. U.S.A.* **107,** 15299–15304